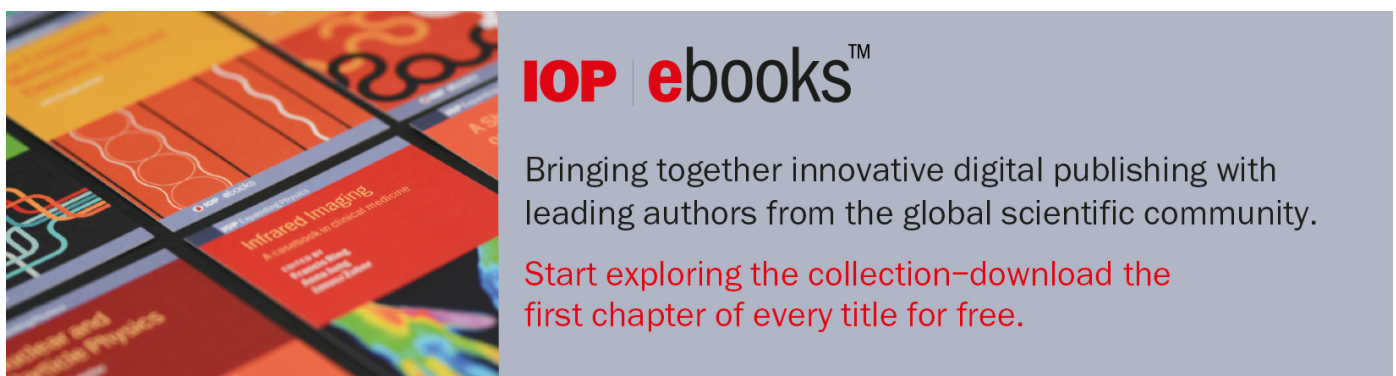


PAPER

Progress in space charge compensation using electron columns

To cite this article: C.S. Park *et al* 2021 *JINST* **16** P03048

View the [article online](#) for updates and enhancements.



IOP | ebooks™

Bringing together innovative digital publishing with leading authors from the global scientific community.

Start exploring the collection—download the first chapter of every title for free.

The advertisement banner features a collage of colorful book covers on the left, including titles like 'Infrared Imaging: A handbook in clinical medicine' and 'Astrophysics and Particle Physics'. The right side has a grey background with the IOP ebooks logo and promotional text.

ICFA BEAM DYNAMICS NEWSLETTER#81 —
ELECTRON LENSES FOR MODERN AND FUTURE ACCELERATORS

Progress in space charge compensation using electron columns

C.S. Park,^{a,*} B. Freemire,^b M. Chung,^c G. Stancari^d and E. Stern^d

^aKorea University, Sejong Campus,
Sejong 30019, South Korea

^bEuclid Techlabs,
Bolingbrook, Illinois 60440, U.S.A.

^cUlsan National Institute of Science and Technology,
Ulsan 44919, South Korea

^dFermi National Accelerator Laboratory,
Batavia, Illinois 60510, U.S.A.

E-mail: kuphy@korea.ac.kr

ABSTRACT: Space charge compensation allows for increased beam current in linacs and RFQs. A novel application of space charge compensation, the electron column, offers the opportunity to realize more intense beams for high energy physics in circular accelerators. The concept relies on ionization of residual gas by the primary beam, with electromagnetic fields used to confine and shape the space charge neutralizing plasma. Prior experimental efforts and simulation studies are reviewed. They indicate that electron columns could be successfully deployed in accelerator rings. The experimental demonstration of an electron column is underway at the Integrable Optics Test Accelerator at Fermilab. The experiment, instrumentation, and physics program are discussed.

KEYWORDS: Accelerator modelling and simulations (multi-particle dynamics; single-particle dynamics); Accelerator Subsystems and Technologies; Beam-line instrumentation (beam position and profile monitors; beam-intensity monitors; bunch length monitors); Beam dynamics

*Corresponding author.

Contents

1	Introduction	1
2	Space charge compensation with electron columns	3
3	Electron column simulations	5
3.1	Fermilab Booster	6
3.2	IOTA	6
4	Prior electron column experiments	9
4.1	INP experiments	9
4.2	Studies with the Tevatron electron lenses	11
5	Electron column experiments in IOTA	11
6	Summary and conclusions	14

1 Introduction

Beam instabilities are one of the major obstacles to achieving high intensities in many accelerators. In particular, space-charge fields, i.e. a beam's own self fields due to Coulomb interactions between particles, can cause beam losses, emittance growth and halo formation. The mitigation of the effects of space charge fields has been a crucial challenge since the birth of accelerators. There have been many proposed methods, such as solenoidal fields to control the beam, beam scrapers to remove halo, and charge neutralization to compensate these forces. For a relativistic beam, the space charge defocusing force is reduced by the magnetic self-field by the factor $1/\gamma^2$.

Charge neutralization, which is the compensation of space charge forces by particles of opposite charge in a plasma, was first introduced by Budker for an electron beam [1]. Charge neutralization can mitigate the space charge effects, and consequently the focusing forces acting on propagating particles can reduce the beam radius and emittance [2]. The degree of the charge neutralization largely depends on residual or injected gas density, gas species, ionization cross section for the generation of non-neutral plasma, beam energy, and the bunch length of the beam. Beam neutralization through residual gas ionization is a common technique in transporting low energy proton or H^- beams in the early stages of RFQs of linear accelerators. However, charge neutralization in circular accelerators largely differs from that in linacs, since the bunch length of the beam in a ring is much shorter and the charge neutralization time is usually large compared to that of betatron oscillations.

Two methods of space charge compensation (SCC) of proton beams in a ring have been considered: the electron lens (EL) and the electron column (EC), and in some cases they may be

combined in a single device. While an EL uses externally injected, low-energy electron beams to achieve a wide range of effects on the circulating beam [3–7], an EC uses the circulating beam itself to ionize the residual gas and to generate the compensating electrons [8–10]. Therefore, electrons in the EC are approximately longitudinally at rest in the lab frame compared to the electron beam in the EL. In both methods, transverse stability of electrons can be provided by strong axial magnetic fields. For more information on ELs for SCC, see also refs. [11, 12]. Although SCC using an EC has not been fully implemented in circular machines, there have been several experimental and computational efforts to study SCC in a ring, showing promising results.

At the Institute of Nuclear Physics (INP, now the Budker Institute of Nuclear Physics) during the 1960s and 1970s, experiments on space charge compensation in a ring with a 1 MeV proton beam were conducted [13–16]. In the 1960s, a hollow copper coil was used as a constant guide field to replace the energy lost during the first few turns after injection, and an axially symmetric magnetic field was applied. While longitudinal instabilities of the beam were observed, the relaxation time of these instabilities was reduced by increasing the residual gas density and injection current. In the 1970s, an electric field was used to replace the beam energy loss caused by gas interactions and the charge-exchange target, clearing electrodes were added to remove secondary charged particles from the circulating beam and two systems for gas leak-in were added to control the gas pressure, but no guiding magnetic field system was used. By increasing the injected gas density, the number of circulating protons was increased, while dipole and quadrupole oscillations of instabilities were quickly damped. These results showed the possibilities of SCC of a bunched beam using ECs in a ring. However, the beam lifetime was reduced as a result of the necessary gas density to prevent beam instabilities. Proper confinement of the plasma electrons (e.g. with a solenoidal magnetic field) should relax the requisite gas density, therefore increasing the beam lifetime.

Y. Alexahin et al. studied the possibility of SCC in the Fermilab Booster ring with ECs [17] as well as ELs [18]. The goal was to increase the proton beam intensity in the Booster ring by more than a factor of two. Initially, it could accommodate only about half the beam intensity from the Fermilab Linac due to strong transverse space charge effects and orbit bump magnets' nonlinearities at injection, which led to fast emittance blowup during bunching. In order to avoid the beta-beat excitations found on simulations with electron lenses, a simulation study of SCC using electron columns was also carried out, especially focused on the required number of electron columns to achieve positive effects. With ECs placed in each of the 24 Booster ring periods, the emittance growth was significantly suppressed. With half the number of columns, compensation was less effective, but still encouraging.

At Fermilab, a series of preliminary experimental studies of space charge compensation using ECs was also carried out [19]. One of the 2-m-long Tevatron Electron Lenses (TELs) installed in the Tevatron collider was converted to an EC by shutting off the electron gun and electron collector of the TEL and by using a 3 T longitudinal magnetic field and two split-cylinder electrodes on both ends. The voltages on electrodes were varied from 0 V to -2 kV. When the 150 GeV proton beam passed the TEL and ionized residual gas, ionization electrons were accumulated and trapped in the column. In this experiment, the tune shift induced by the compensation was observed. However, it was less than half of the analytically calculated prediction. With low vacuum pressure, there were significant vacuum instabilities, which led to emittance growth and beam loss. In order to understand these unexpected phenomena, another experimental study was conducted at the Fermilab

Electron Lens Test Stand, which was operated with electron beams rather than a proton beam. This study showed accumulation of negative charge between electrodes with negative voltages.

The Integrable Optics Test Accelerator (IOTA) at the Fermilab Accelerator Science and Technology (FAST) facility is aimed at implementing nonlinear integrable lattices, which could improve beam instabilities due to periodic perturbations and mitigate collective effects through Landau damping [20]. Studies of space charge compensation using the electron lens and the electron column schemes are also planned in the IOTA ring. Both SCC methods require precise control of the density and distribution of the compensating electrons using a solenoid and electrodes. Prior to implementation of the SCC experiments in IOTA, simulations of the EC have been performed using Warp (EC only, refs. [21–24]) and Synergia (including the IOTA ring, ref. [25]). The initial approach for the simulations was to understand the physical processes of charge neutralization inside the column and to estimate the parameter ranges of the solenoidal magnetic field, voltages on the electrodes, and gas pressure for SCC. A coasting beam was considered first, and then a beam with a finite bunch length was used.

The physics goals of the electron column experiment in IOTA are to characterize the generation and evolution of the non-neutral plasma forming the column utilizing plasma diagnostics, and to measure the space charge compensation effects on the beam emittance, size, lifetime and tune shift. In contrast to the previous experiments, precise control of the electron density and distribution using a solenoid and electrodes, together with better diagnostics, is expected to improve the degree of SCC and suppress electron-proton ($e-p$) and vacuum instabilities.

In this paper, we describe the physics of space-charge compensation with electron columns, review previous experiments and numerical simulations, and outline the future research program in IOTA.

2 Space charge compensation with electron columns

Space charge compensation using electron columns is a method to achieve charge neutralization of positive ion beams by trapping electrons, produced from ionization of the residual gas by the ion beam itself. The ionization electrons can be confined inside the column and their distributions controlled with a solenoid magnet and electrodes.

The EC method was studied experimentally and numerically for various accelerators before. However, beam instabilities were not fully suppressed, beam lifetime was poor, and plasma confinement was not fully implemented, as mentioned above [13–19]. An electron column layout to overcome these issues was proposed [9, 10]. This EC setup consists of a solenoid magnet, confining electrodes (ring- or cylinder-shaped) at both ends of the column, electron collectors, and vacuum ports for differential pumping (figure 1). The advantages of this concept are not only to trap electrons inside the column for charge neutralization, but also to control and match the electron density profiles to those of the propagating positive ion beam.

Space charge compensation via charge neutralization can be characterized by a neutralization time τ_N — the time required for the electron charge density to match that of the beam. Assuming only ionization by the beam and no recombination, the variation of the electron density with time is

$$\frac{dn}{dt} = n_b n_g \sigma_i v, \quad (2.1)$$

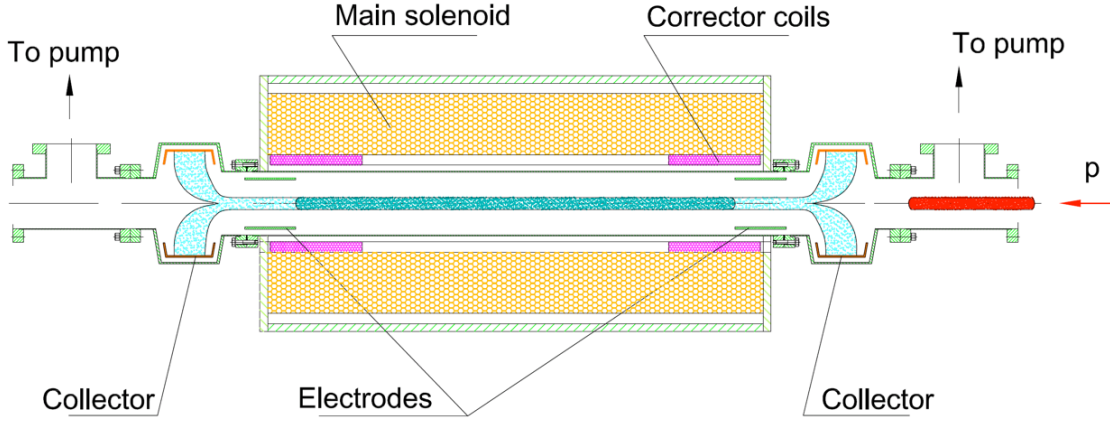


Figure 1. Schematic layout of the electron column experimental setup.

where n_b is the beam density, n_g the gas density, σ_i the ionization cross section, and v the beam velocity. The neutralization time [2] is given by

$$\tau_N = \frac{1}{n_g \sigma_i v}, \quad (2.2)$$

if there is no external magnetic field.

For proton beams, the impact ionization cross section, which depends on the beam velocity and on the atomic properties of the gas species, can be expressed in the following combined form [26]:

$$\sigma_i = \left(\frac{1}{\sigma_l} + \frac{1}{\sigma_h} \right)^{-1}, \quad (2.3)$$

where σ_l and σ_h are the cross sections corresponding to the low- and high-energy regions, respectively. For proton beam kinetic energies $T_b > 5$ MeV, $\sigma_l \gg \sigma_h$ and $\sigma_i \approx \sigma_h$. For the case of hydrogen, σ_l and σ_h are empirically approximated by

$$\begin{cases} \sigma_l = 3.575 \times 10^{-15} \beta^{2.48}, \\ \sigma_h = \frac{1.872 \times 10^{-24}}{\beta^2} [0.71 \ln(1 + 1.879 \times 10^4 \beta^2) + 1.63] & \text{for } T_b < 5 \text{ MeV,} \\ \sigma_h = \frac{1.329 \times 10^{-24}}{\beta^2} [\ln(1.866 \times 10^5 \beta^2 \gamma^2) - \beta^2] & \text{for } T_b \geq 5 \text{ MeV,} \end{cases} \quad (2.4)$$

where β and γ are the relativistic factors.

In the case of the 2.5 MeV proton beam in IOTA, σ_i is approximately $1.73 \times 10^{-21} \text{ m}^2$. If the gas pressure is $p = 5 \times 10^{-4} \text{ torr}$, the gas density is $n_g = (3.54 \times 10^{22} \text{ m}^{-3} \cdot \text{torr}^{-1}) \times p = 1.77 \times 10^{19} \text{ m}^{-3}$, and the neutralization time is $\tau_N = 1.5 \mu\text{s}$. For comparison, the revolution period of protons in IOTA will be $\tau = 1.83 \mu\text{s}$. As the cross section and beam velocity are fixed, the gas density will determine the neutralization time for the beam. This predicates good control over the gas injection and pump out systems. Depending on the time scale of the evolution of instabilities (due to space charge or impedances, for instance), neutralization over several turns may be sufficient, relaxing the requirements on residual gas pressure.

A positively charged ion beam naturally expels ions and attracts electrons. To some degree, this counteracts the thermal drift of the electrons. If an external magnetic field is applied, both the electrons and ions will experience a $\vec{E} \times \vec{B}$ drift. For the case of a solenoidal field, due to their smaller mass, electrons will be more strongly confined than ions. Therefore, the magnetic field should be weak enough to allow ions to escape from the column to avoid their degrading effect on SCC (through recombination with electrons or their own positive electric charge), but also strong enough to trap the electrons transversely. This external magnetic field also suppresses e - p instabilities.

A pair of electrodes can control the longitudinal confinement and accumulation of electrons inside the column. The beam potential on axis for a flat current-density distribution is $\phi = I_b / (4\pi\epsilon_0 c\beta) = (30 \text{ V/A}) I_b / \beta$, and similar expressions apply for other distributions. The voltage applied to the electrodes should be of a similar magnitude to tune the confinement of the electrons and to avoid overcompensation. For instance, for the maximum proton beam current of 8 mA in IOTA, the beam potential is approximately $\phi = 3.3 \text{ V}$. The matched condition for SCC found in simulations is a voltage of about -5 V on the confining electrodes.

In the ideal compensation conditions, the distributions of confined electrons and circulating beam should be matched both transversely and longitudinally.

3 Electron column simulations

The effect of one or more electron columns has been simulated for several accelerators. The level of complexity and number of physical processes included in the simulations has improved over time. There are three main impediments in implementing a complete end-to-end simulation: the differing time scales involved, the number of simulated particles, and plasma generation and evolution. If the EC is treated as an object of non-zero length (i.e. not a simple electrostatic lens), then the smallest time scale is often the cyclotron period of plasma electrons in the solenoidal magnetic field. For the case of the 0.1 T field planned for the IOTA implementation of an EC, this corresponds to about 0.35 ns. This is several orders of magnitude less than the revolution period of many circular machines, for example $\sim 2 \mu\text{s}$ for both the Booster and IOTA at Fermilab. This results in a computationally intense simulation if the interaction between the beam, gas and plasma is to be included over many turns. The computational burden also obviously increases with the number of simulation particles. A large number of particles is desirable for two reasons: first, for experiments in which the tails of the beam are of great interest, such as in IOTA, a sufficient number of simulated beam particles are required to sufficiently resolve the halo and track its evolution; second, in order to avoid localized regions of artificially high charge within the plasma, a sufficient number of simulated plasma particles are needed. This is true for both plasma electrons and ions. In addition to the sheer number of plasma particles needed to produce a realistic result, handling of charge is important: from production to tracking to removal. This is primarily an issue to be addressed in the simulation framework, but contains complex issues — where macro-particles are placed when created, how to address charged particle collisions, and how to handle recombination and particle losses. To date, creating the plasma and tracking particles have been handled reasonably well. However, accounting for processes such as collisional energy loss or recombination of electrons and ions have yet to be

taken into account in simulation. Some of the results of the efforts to simulate electron columns are summarized below.

3.1 Fermilab Booster

Fast emittance blowup during bunching was predicted to occur in the Fermilab Booster as a result of increasing the number of protons per bunch [18]. It was shown that the addition of one or two electron lenses resulted in poor particle dynamics, which was conjectured to be due to beta-beat excitation. To overcome these detrimental perturbations while compensating space charge, a study of the number of electron columns needed was performed [17].

Simulations were done using Mathematica and MAD [27], and the ECs were implemented as equidistant thin beam-beam elements with transverse sizes equivalent to the beam size at the location of the column. The simulations were in two dimensions, with synchrotron motion only taken into account when calculating the bunching factor. The number of columns as well as the space charge compensation factor (a number between 0 and 1, corresponding to the degree by which the charge in the column matched that of the beam) were varied, and particles tracked over 200 turns.

With no space charge compensation, the emittances grew by 50% to 100%. With a 50% compensation factor, the emittances grew by 10% to 15%, and with a 100% compensation factor, the emittances decreased slightly for the nominal bunch intensity. At higher bunch intensities, simulations indicated that the ECs were still beneficial at decreasing the final emittances with a large number of columns.

3.2 IOTA

The simulation package for the electron column to be implemented in IOTA has grown from initially using Warp [28, 29] to model only the section of the ring containing the main solenoid, to include modeling the entire IOTA ring in Synergia [30, 31], as well as improved physics processes and beam parameters in Warp. Figure 2 shows the first simulation of the EC in IOTA using Warp. A longitudinally continuous (i.e. coasting, unbunched) beam was considered, with a solenoid used to confine electrons transversely, and electrodes used for longitudinal confinement. Electrons can be seen to be well confined within the radius of the beam and length of the solenoid, while ions escape at the ends of the solenoid. This early work demonstrated that plasma production and confinement were possible within the framework of Warp.

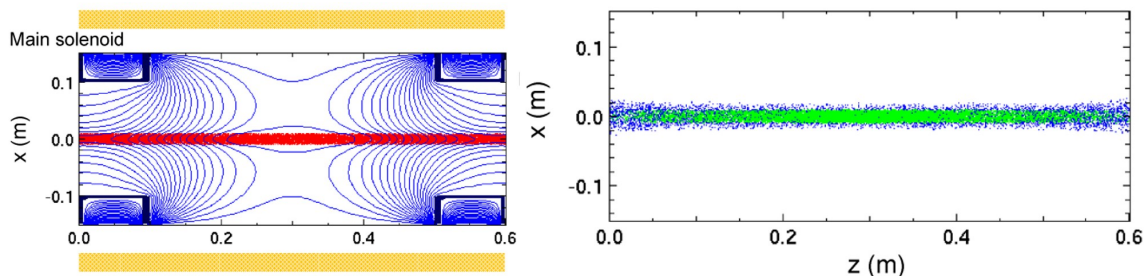


Figure 2. Simulated particle distributions from the first-generation Warp model of the IOTA EC: protons (red), positive ions (blue) and electrons (green). Reproduced from ref. [21].

For space charge compensation to be effective, the density and profile of the neutralizing electron plasma should match those of the positively charged beam (protons in the case of IOTA). As the EC relies on passive generation of the neutralizing plasma — through ionization of background gas by the beam — one must study both the generation of the proper electron profile and its evolution over time. Using Warp to perform 3D simulations, the confining external magnetic and electric fields and the background gas pressure were optimized so that the transverse and longitudinal density profiles of the plasma electrons closely matched those of the proton beam [22]. A coasting beam was used for these simulations. Figure 3 shows the simulated average electron density and proton beam density plotted as a function of time for various solenoid and electrode strengths. The parameters that were found to produce matched transverse and longitudinal profiles were $B = 0.1$ T, $V = -5$ V, and $p = 5 \times 10^{-4}$ torr. The resulting simulated density profiles for these parameters are shown in figure 4. For a given solenoid field, the neutralization time decreased as the voltage on the electrodes was reduced.

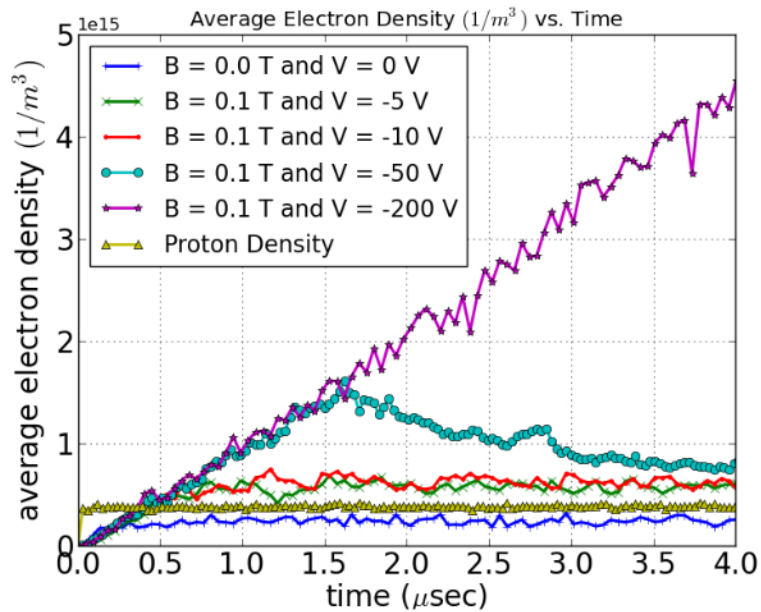


Figure 3. Simulated average electron density vs. time for the IOTA EC. Colored datasets correspond to different solenoid and electrode strengths. The proton beam density is shown in yellow. Reproduced from ref. [22].

To further improve the simulation accuracy, the time structure of the IOTA proton beam was taken into consideration. The evolution of the EC plasma was studied over the course of two passes of the bunched beam [23, 24]. This was important in both estimating the beam equilibrium emittance once the plasma reached a steady state, and in predicting potential beam instabilities (e - p , for example). Additionally, processes such as ion formation ($H_2^+ + H_2 \rightarrow H_3^+ + H$) and electron energy spread were added to improve the plasma physics model. The transverse distribution of protons, electrons and ions at the center of the EC, just before the beam exited after the first pass (the beam pulse length was $1.77 \mu\text{s}$), are shown on the left in figure 5. The electron distribution matches that of the beam. However, the density has not yet reached that of the beam. The ions,

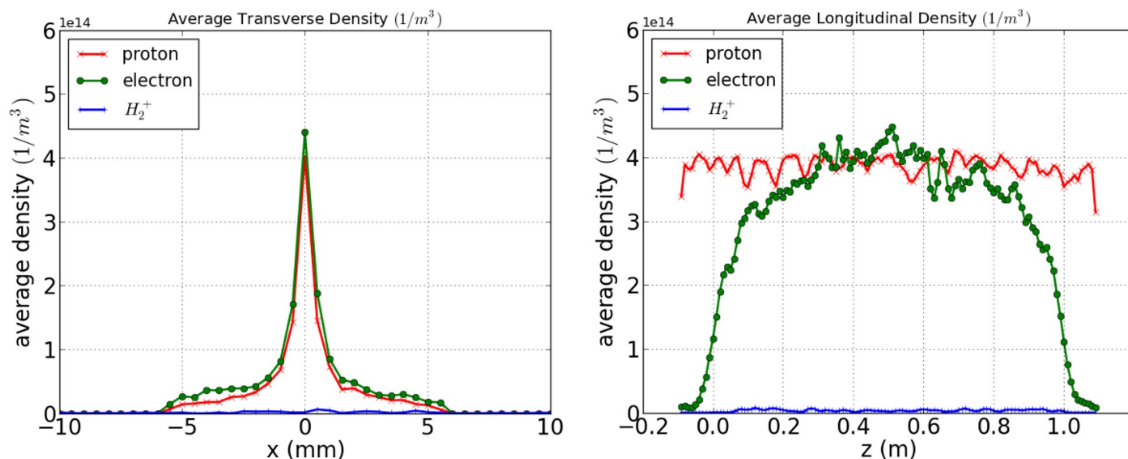


Figure 4. Transverse (left) and longitudinal (right) density profiles for the proton beam (red), electrons (green), and positive hydrogen ions (blue), with simulated parameters $B = 0.1$ T, $V = -5$ V, and $p = 5 \times 10^{-4}$ torr. Reproduced from ref. [22].

not as confined by the magnetic field as the electrons, migrate outward radially. The plot on the right of figure 5 illustrates the achieved degree of space charge compensation. The ratio of the radial component of the electric field with space charge compensation to that with no space charge compensation is plotted. The sharp peak at the center is due to the electric field being zero at the very center of the beam, while there is a small field at the center of the plasma column (the SCC case) as a result of ion drift, thermal motion, etc. Disregarding this artifact, a $\sim 50\%$ reduction in the electric field is achieved after the second pass through the EC.

To incorporate the rest of the IOTA ring, the lattice for the electron lens case as implemented in MAD-X [32] was used to simulate the IOTA ring with Synergia [25]. To achieve optimum space charge compensation, the betatron functions for horizontal and vertical directions should be equal at the location of the EC and there should be no dispersion. The momentum spread of the proton beam coming out of the RFQ is expected to be large enough ($\sim 0.1\%$) that the beam will completely fill the ring within a short time [20]. A single RF cavity was adiabatically ramped to produce four bunches. A single bunch was generated with a Gaussian transverse distribution, uniform longitudinal distribution, and normal momentum spread based on the expected value out of the RFQ. The bunch was tracked for 10,000 turns, with the RF ramp taking 1,400 turns. The effectiveness of the bunching procedure was evaluated without space charge or aperture restrictions. Figure 6 shows the longitudinal phase space initially and after the RF ramp is complete. With space charge and a 25.4 mm aperture radius, significant beam loss occurred, with less than 10% of particles surviving 10,000 turns. The initial and final transverse (x - y) distributions and RMS emittance growth are shown in figure 6. These simulations were done without the EC, demonstrating the drastic effect space charge has on the uncompensated beam in IOTA.

To date, simulations of the electron column implemented in Warp and of the IOTA ring implemented in Synergia have been completed separately. Synergia simulations cover the beam bunching process, space charge and aperture losses. Warp simulations describe the bunched beam passing through the EC multiple times, with the plasma tracked throughout this time. Integrating

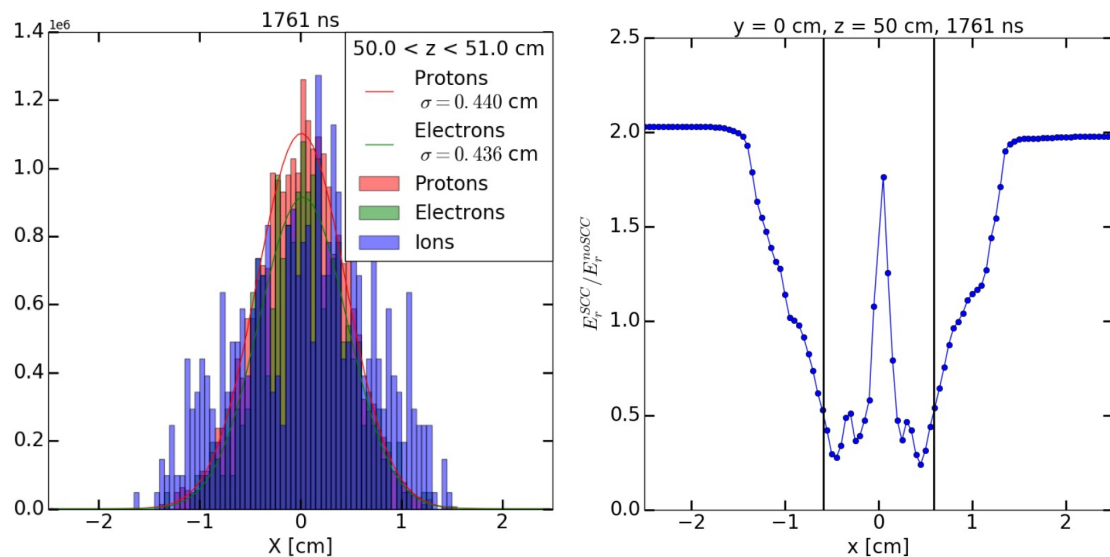


Figure 5. Left: transverse distribution of protons (red), electrons (green), and positive ions (blue) at the center of the EC just before the beam exits after the first pass. Reproduced from ref. [23]. Right: ratio of the radial component of the electric field with space charge compensation to that without space charge compensation, plotted in one transverse dimension. The vertical lines denote the size of the beam. Reproduced from ref. [24].

these two complementary calculation frameworks is an outstanding task that needs to be addressed.

4 Prior electron column experiments

Space charge compensation via ionization of residual gas was first introduced in the 1950s [1], with the first experiments to attempt SCC occurring in the 1960s and 1970s [13–15]. This was followed by an experiment at Fermilab utilizing one of the Tevatron electron lenses [19].

4.1 INP experiments

The first experiments to test the effect of space charge compensation on a stored proton beam occurred at the Institute of Nuclear Physics [13–15].

During the first set of experiments, protons with currents up to $300\ \mu\text{A}$ were injected into a storage ring via the charge-exchange method [13]. A hollow copper coil was used as a guide field and to replace energy loss during injection. The nominal hydrogen gas pressure was 5×10^{-5} torr and the first experiments were carried out with an axially symmetric magnetic field. At maximum injection current, 5×10^{10} protons could be stored. However, longitudinal instabilities resulted. Attempts to increase the number of stored protons by increasing the gas pressure (up to 10^{-3} torr) resulted in beam loss due to a vertical beam instability.

The second set of experiments involved injecting protons via charge-exchange up to 8 mA into a racetrack-style storage ring [15]. The magnetic flux from a betatron core produced an azimuthal electric field across an accelerating gap to replace beam energy loss due to interaction with the gas and the charge-exchange target. Gas was injected into the ring via two methods: a system of four

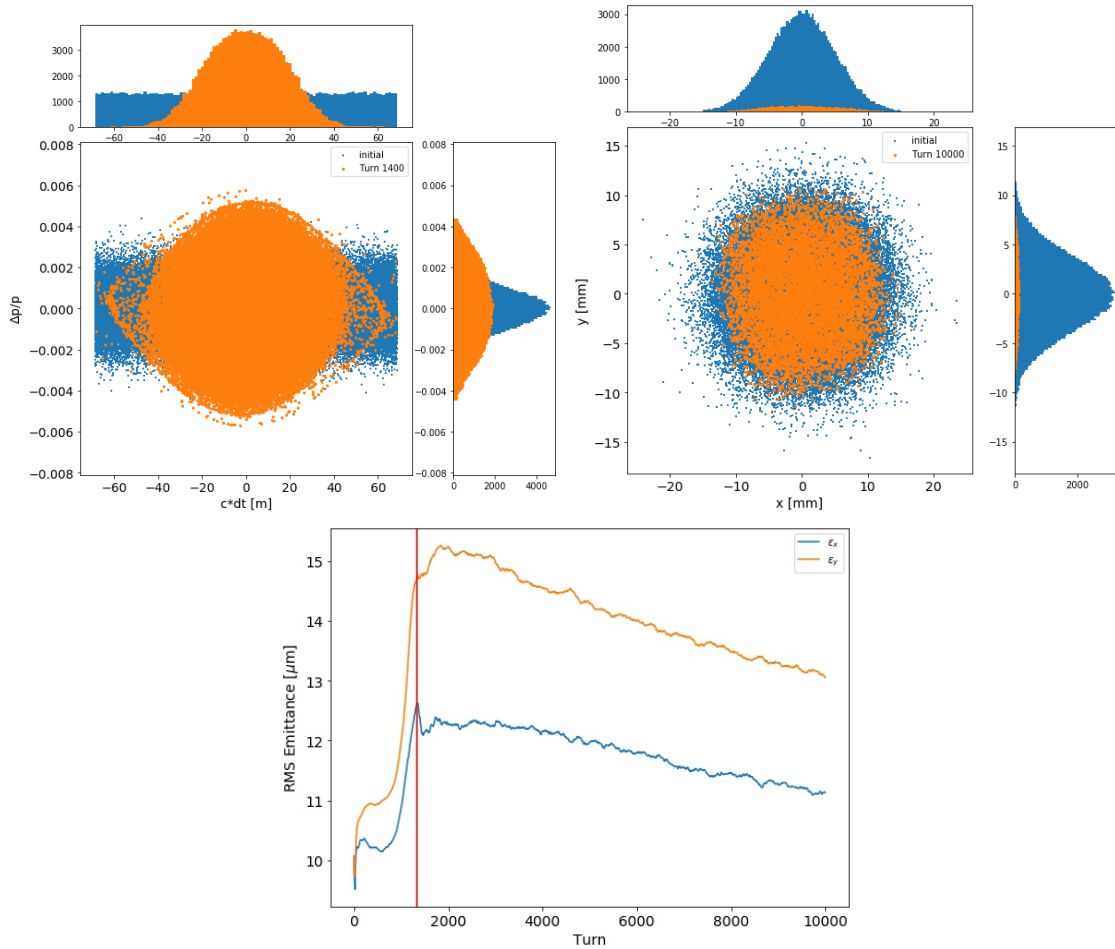


Figure 6. Longitudinal phase space initially (blue) and after the RF ramp is complete (orange) without space charge or an aperture — top left. Transverse x - y beam distribution initially (blue) and after 10,000 turns (orange) with space charge and an aperture — top right. RMS emittance growth for x (blue) and y (orange) over 10,000 turns with space charge and an aperture — bottom. The vertical red line corresponds to the end of the RF ramp. Reproduced from ref. [25].

stationary leaks which allowed for a homogeneous distribution of gas, and a system of four pulsed valves which allowed for a density distribution to be achieved. Electrodes were placed around the ring to clear ionization products.

Measurements were taken with the electrodes on and off, with no additional gas injected into the ring, as a baseline. It was found that $\sim 1.9 \times 10^{11}$ protons could be stored with the electric clearing field. Without the clearing field, the beam lifetime decreased by more than a factor of two, due to intense coherent vertical beam oscillations.

A series of measurements were then taken by injecting various gases to achieve different residual gas pressures in the ring, and studying the effect on the beam stability and lifetime. It was found that for low residual gas pressures, increasing pressure resulted in larger beam instability and hence fewer stored protons. Above a certain residual gas pressure, oscillations in the beam quickly damped, and the number of stored protons generally increased with pressure.

The time dependence of the number of ions in the beam region was also studied. The quantity $N_i/(n_g N_p v_p)$, where N_i and N_p are the number of ions and protons, respectively, n_g is the gas density, and v_p is the proton velocity, gives an indication of the rate at which the total number of ions is changing, the derivative being the effective collection cross section, i.e. the difference between the production rate and loss rate. The estimated ionization cross section for nitrogen at 3.6×10^{-4} torr (above the threshold for beam oscillation damping) is 5×10^{-16} cm², which is approximately three times larger than the ionization cross section of nitrogen by 1 MeV protons. The proposed reason for the increased production rate was that plasma electrons contributed significantly to ionization above the threshold pressure for each gas. This mechanism generated the threshold above which the beam became stable. Below the threshold pressure for each gas, the effect of space charge limited the number of stored protons. Near the threshold pressure, unstable beam oscillations were observed, with the instability stabilizing as the density of the plasma electrons reached that of the beam. Above the threshold pressure, i.e. the plasma electron and beam densities being equal, the amplitude and duration of beam oscillations decreased and the beam became stable. However, as a result of the multiple scattering off the high density residual gas, the beam lifetime also decreased. In this regime, the measured beam potential was 10–30 V, compared to the 200 V measured without residual gas injection. The achieved number of stored protons ranged from 0.75×10^{12} to 1.25×10^{12} , depending on gas species, almost an order of magnitude increase from the uncompensated case. When an accelerating voltage was applied to the beam to compensate energy loss, the lifetime and number of stored protons increased. The maximum beam lifetime and population achieved were 120 revolutions and 1.8×10^{12} protons.

4.2 Studies with the Tevatron electron lenses

Two electron lenses were operated in the Tevatron at Fermilab [4]. One of the lenses was configured similarly to the layout shown in figure 1, and studies were done to evaluate its effect on a 150 GeV proton beam [19]. A superconducting solenoid provided a 3 T longitudinal field over 2 m. The electron gun and collector used for the lens were grounded during measurements, to ensure no external electron current was introduced. The voltages on opposing split-cylinder electrodes were operated between 0 V and -2 kV to provide longitudinal confinement of the electrons. As opposed to the experiments done at INP, those done in the Tevatron could not utilize the injection of gas into the beam pipe, but rather relied on accumulated ionization electrons from residual gas trapped by the electric and magnetic fields.

Measurements made at the nominal vacuum pressure of 3×10^{-9} torr resulted in no observable tune shift, regardless of the electrode voltage. When the vacuum was degraded to 5×10^{-8} torr, by either heating the vacuum chamber or by running current from the electron gun into the walls of the vacuum chamber, a positive tune shift was measured. The predicted value was more than twice the measured value, which was not explained. Additionally, vacuum instabilities occurred during the measurements, which drove beam instabilities, resulting in emittance growth or beam loss.

5 Electron column experiments in IOTA

Understanding and control of high-intensity beams is one of the main purposes of the IOTA/FAST research program [11, 20]. Electron columns are an essential component of this program.

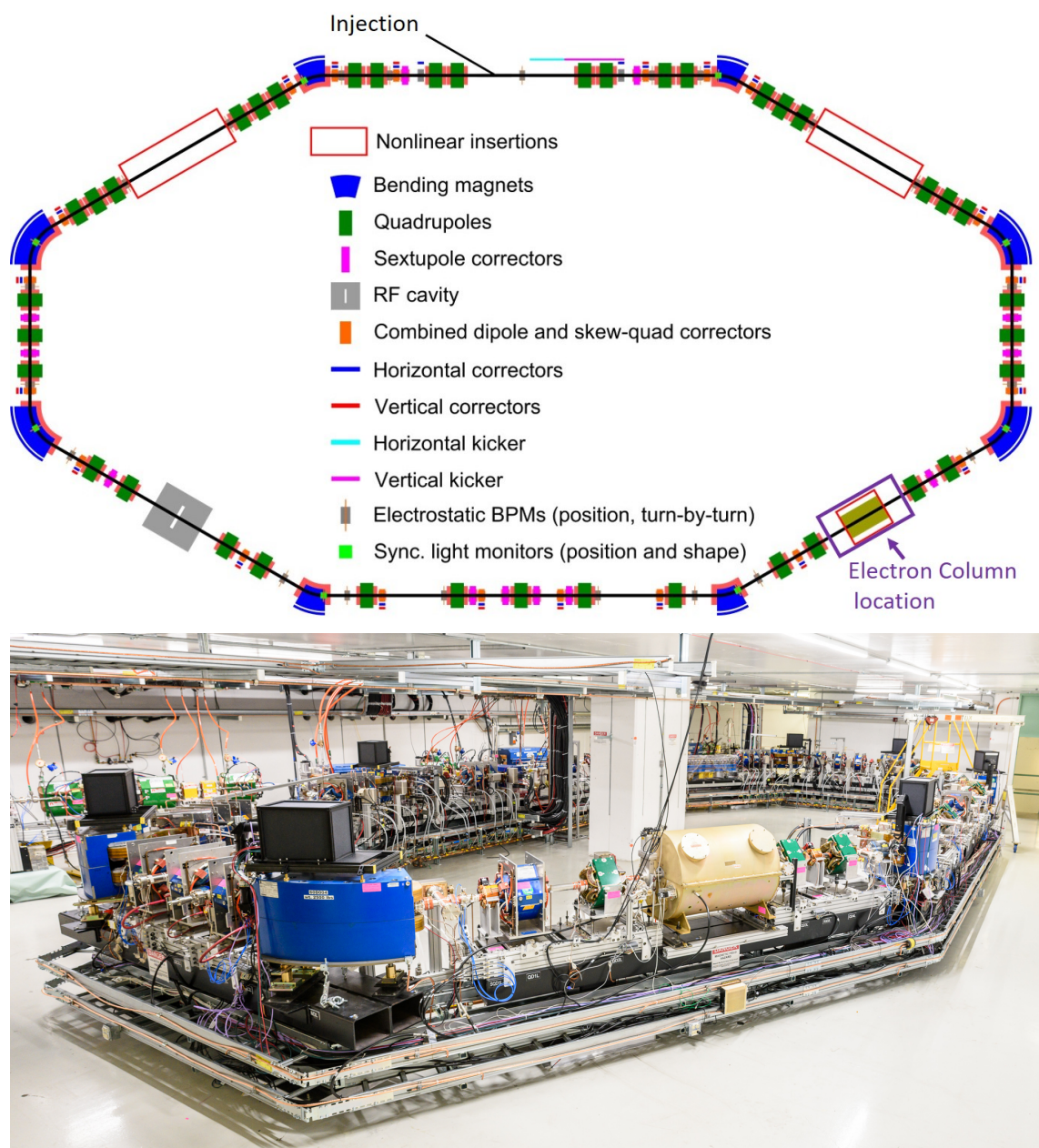


Figure 7. Schematic of the IOTA ring (top). The planned location of the EC is outlined in purple. Photograph of the IOTA ring as of November 2018 (bottom), with a bending magnet (blue) and the RF cavity (gold) in the foreground. (Photo: Giulio Stancari)

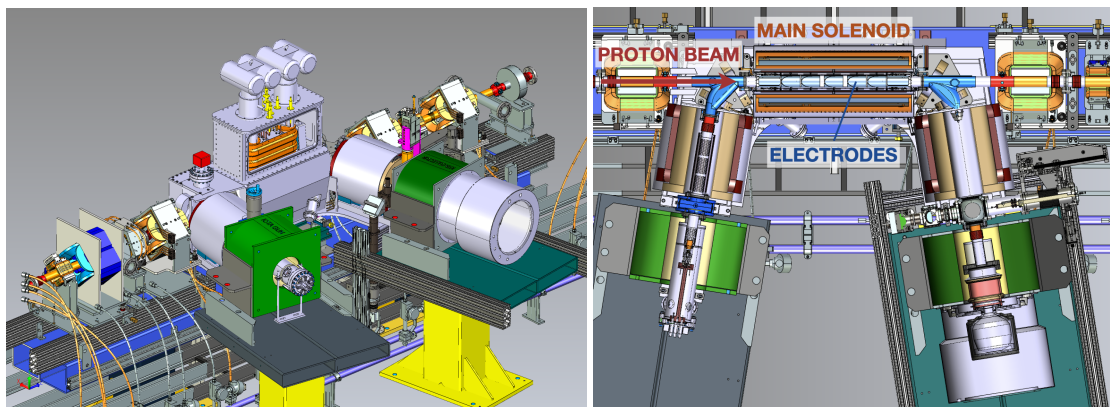


Figure 8. Isometric view of the IOTA electron lens beamline section (left) and top cutaway view (right). Design developed in collaboration with D. Perini and A. Kolehmainen of the CERN Mechanical Engineering team.

IOTA is a 40 m circumference storage ring dedicated to beam physics research (figure 7). The ring can store electrons with kinetic energies of 150 MeV or protons at 2.5 MeV. Electrons were circulated for the first time in August 2018. The experimental runs typically last for a few months, separated by maintenance and installation periods. Currently, IOTA Run 3 is under way. Installation and commissioning of the IOTA proton injector is planned for the end of 2021. It will provide 2.5 MeV protons with intensities up to 8 mA, opening up opportunities for research with space-charge-dominated beams. The IOTA focusing lattice is flexible and has straight sections to accommodate a range of modular experiments, such as nonlinear magnets for integrable optics, optical stochastic cooling, or electron lenses.

An EC layout similar to that shown in figure 1 is being designed and incorporated in the functions of the IOTA electron lens [11, 20]. The current design is shown in figure 8.

The EC experiments must focus on both the control of the electron plasma and on the effects on the proton beam. These are the main opportunities and challenges of EC studies in IOTA. Characterization of the plasma relies on diagnostics. Pickup electrodes will provide information on the intensity and frequency spectrum of plasma oscillations. The current on biased electrodes will measure the flux of lost ions and electrons. The use of a pickup antenna to sense cyclotron radiation and monitor the electron plasma density and temperature (besides providing a very accurate measurement of the magnetic field) was applied to electron cooling [33–35] and to other precision measurements [36–38]. We plan to include this type of detector in the apparatus. The experimental conditions can be varied by changing the solenoid field strength, the electrode potentials and the residual gas pressure. The main effect on the proton beam is of course lifetime, measured with the IOTA direct-current current transformer (DCCT) and wall current monitor (WCM). The WCM can also monitor the proton pulse longitudinally. The range of 2.5 MeV protons in metal is smaller than the beam pipe thickness and losses can only be monitored inside the vacuum chamber. Prototype in-vacuum diamond detectors have been used in other machines [39, 40] and are being considered for proton loss measurements in IOTA as well.

Continuous monitoring of proton transverse profiles and emittances is challenging and various options are being considered. A compact gas-sheet profile monitor (GSPM) was built and char-

acterized [41, 42]. Tests on a cyclotron beamline at the Crocker Nuclear Laboratory are planned before installation in IOTA. Another option is the detection of neutral hydrogen from recombination. The maximum recombination rate is achieved when proton and electron velocities are matched. A neutralization monitor based on microchannel plates and a phosphor screen, installed downstream of the first dipole after the IOTA electron lens, will be used to tune the electron lens as an electron cooler [43]. Although the recombination rate in the EC configuration will probably be too low for fast profile measurements, the system can be used to monitor proton-plasma interactions.

One of the most challenging aspects of the EC experimental program is the gas injection system. Ideally, one would like to vary the local residual gas pressure over a wide range, to control the neutralization times and plasma densities, ensuring acceptable vacuum levels in the rest of the ring and reasonable beam lifetimes. Whether the injection system can be integrated in the present design of the IOTA electron lens or whether a separate system is necessary is still an open question.

Research at IOTA provides novel experimental conditions for the study of space charge compensation in rings. The development of the scientific program is in an active stage, with several opportunities for collaboration.

6 Summary and conclusions

The physics and the applications of space charge compensation in rings have been described. Early attempts at space charge compensation of a proton beam in a ring were moderately successful — the number of stored particles could be increased at the cost of the lifetime of the beam. An improved concept, the electron column, was proposed, which utilizes electric and magnetic fields to trap and shape the plasma generated when a beam ionizes a section of residual gas. Electron column experiments were first attempted adapting one of the electron lenses in the Fermilab Tevatron collider. A simulation program was launched in order to understand the evolution of the generated plasma and its effects on hadron beams. The results will be used as the basis for a dedicated experimental program at the Integrable Optics Test Accelerator at Fermilab. The experiment, instrumentation, and physics program were outlined. The main goals are to advance the understanding of these systems and to provide experimental demonstrations of the concept that will allow hadron circular accelerators to reach higher beam intensities and brightnesses.

Acknowledgments

The authors are very thankful to S. Chattopadhyay, C. Mitchell, G. Penn, A. Romanov, R. Ryne, V. Shiltsev, C. Thangaraj and A. Valishev for useful discussions on the physics of space charge compensation and on the design of the IOTA ring. This manuscript has been authored by Fermi Research Alliance, LLC under Contract No. DE-AC02-07CH11359 with the U.S. Department of Energy, Office of Science, Office of High Energy Physics. This work was supported by the National Research Foundation of Korea (NRF) grant funded by the Korea Government (MSIT) (No. 2020R1A2C1014675), and the U.S. Department of Energy, Office of High Energy Physics, General Accelerator Research and Development (GARD) Program. Synergia development has been supported by the U.S. Department of Energy, Office of Science, Office of Advanced Scientific

Computing Research and Office of High Energy Physics, Scientific Discovery through Advanced Computing (SciDAC) program.

References

- [1] G. I. Budker, *Relativistic stabilized electron beam*, *Sov. J. Atom. Energy* **1** (1956) 673.
- [2] M. Reiser, *Theory and Design of Charged Particle Beams*, Wiley-VCH (2008).
- [3] V. Shiltsev, Y. Alexahin, V. Kamerzhiev, G. Kuznetsov, X.-L. Zhang and K. Bishofberger, *Experimental demonstration of compensation of beam-beam effects by electron lenses*, *Phys. Rev. Lett.* **99** (2007) 244801 [[arXiv:0705.0320](https://arxiv.org/abs/0705.0320)].
- [4] V. Shiltsev et al., *Tevatron electron lenses: Design and operation*, *Phys. Rev. ST Accel. Beams* **11** (2008) 103501 [[arXiv:0808.1542](https://arxiv.org/abs/0808.1542)].
- [5] G. Stancari, A. Valishev, G. Annala, G. Kuznetsov, V. Shiltsev, D.A. Still et al., *Collimation with hollow electron beams*, *Phys. Rev. Lett.* **107** (2011) 084802 [[arXiv:1105.3256](https://arxiv.org/abs/1105.3256)].
- [6] W. Fischer et al., *Operational head-on beam-beam compensation with electron lenses in the Relativistic Heavy Ion Collider*, *Phys. Rev. Lett.* **115** (2015) 264801.
- [7] V.D. Shiltsev, *Electron Lenses for Super-Colliders*, Springer (2016), DOI: [10.1007/978-1-4939-3317-4](https://doi.org/10.1007/978-1-4939-3317-4).
- [8] A. Burov, G.W. Foster and V.D. Shiltsev, *Space-charge compensation in high-intensity proton rings*, Tech. Rep., FNAL-TM-2125, Fermilab (2000).
- [9] V. Shiltsev, *On possibility to compensate space charge effects by controlled electron columns*, Tech. Rep., FNAL-Beams-doc-2810-v1, Fermilab (2007).
- [10] V. Shiltsev, *New possibilities for beam-beam and space-charge compensation: MCP gun and electron columns*, in proceedings of *Particle Accelerator Conference*, Albuquerque, NM, U.S.A., 25–29 June 2007, pp. 1159–1160.
- [11] G. Stancari et al., *Beam physics research with the IOTA electron lens*, in *ICFA Beam Dynamics Newsletter #81* (2021).
- [12] E. Stern et al., *Self-consistent PIC Simulations of Ultimate Space Charge Compensation with Electron Lenses*, in *ICFA Beam Dynamics Newsletter #81* (2021).
- [13] G.I. Budker, G.I. Dimov, V.G. Dudnikov, A.A. Sokolov and V.G. Shamovsky, *Experiments on electron compensation of proton beam in ring accelerators*, in proceedings of the 6th *International Conference on High Energy Accelerators*, Cambridge, Massachusetts, U.S.A., 11–15 September 1967, pp. A103–A105.
- [14] Y. Bel’chenko, G. Budker, G. Derevyankin, G. Dimov, V. Dunikov, G. Roslyakov et al., *High-current proton beam developments in Novosibirsk*, in proceedings of the 10th *International Conference on High Energy Accelerators*, Protvino, USSR, 11–17 July 1977, pp. 287–294.
- [15] G. Dimov and V. Chupriyanov, *Compensated proton-beam production in an accelerating ring at a current above the space-charge limit*, *Part. Accel.* **14** (1984) 155.
- [16] V. Dudnikov, *Condition for production of circulating proton beam with intensity greater than space charge limit*, *AIP Conf. Proc.* **642** (2002) 367.
- [17] Y. Alexahin and V. Kapin, *Study of possibility of space charge compensation in the Fermilab Booster with multiple electron columns*, Tech. Rep., FNAL-Beams-doc-3108-v1, Fermilab (2008).

- [18] Y. Alexahin, A. Drozhdin, N. Kazarinov and X. Yang, *Effects of space charge and magnet nonlinearities on beam dynamics in the Fermilab Booster*, in proceedings of *Particle Accelerator Conference*, Albuquerque, NM, U.S.A., 25–29 June 2007, pp. 3474–3476.
- [19] V. Shiltsev, A. Valishev, G. Kuznetsov and V. Kamerzhiev, *Beam studies with electron columns*, in proceedings of *Particle Accelerator Conference*, Vancouver, BC, Canada, 4–8 May 2009, pp. 3233–3235.
- [20] S. Antipov et al., *IOTA (Integrable Optics Test Accelerator): Facility and experimental beam physics program*, 2017 *JINST* **12** T03002 [[arXiv:1612.06289](https://arxiv.org/abs/1612.06289)].
- [21] M. Chung, L. Prost and V.D. Shiltsev, *Space-charge compensation for high-intensity linear and circular accelerators at fermilab*, in proceedings of *Particle Accelerator Conference*, Pasadena, CA, U.S.A., 29 September–4 October 2013, pp. 402–404.
- [22] C.S. Park, V.D. Shiltsev, G. Stancari, J.C.T. Thangaraj and D. Milana, *Space charge compensation using electron columns and electron lenses at IOTA*, in proceedings of *North America Particle Accelerator Conference*, Chicago, IL, U.S.A., 9–14 October 2016, pp. 1257–1259.
- [23] B. Freemire, S. Chattopadhyay, V.D. Shiltsev, G. Stancari, C.S. Park, G. Penn et al., *Simulations of the electron column in IOTA*, in proceedings of *International Particle Accelerator Conference*, Vancouver, BC, Canada, 29 April–4 May 2018, pp. 1103–1106.
- [24] B. Freemire, S. Chattopadhyay, V.D. Shiltsev, G. Stancari, C.S. Park, G. Penn et al., *Space-charge compensation using electron columns at IOTA*, in proceedings of the *61st ICFA Advanced Beam Dynamics Workshop on High-Intensity and High-Brightness Hadron Beams*, Daejeon, South Korea, June 2018, pp. 247–251.
- [25] B. Freemire, S. Chattopadhyay, E.G. Stern, C.S. Park, C.E. Mitchell, R.D. Ryne et al., *Multipass simulations of space charge compensation using an electron column at IOTA*, in proceedings of *International Particle Accelerator Conference*, Melbourne, Australia, 19–24 May 2019, pp. 3313–3316.
- [26] M.E. Rudd, Y.K. Kim, D.H. Madison and J.W. Gallagher, *Electron production in proton collisions: total cross sections*, *Rev. Mod. Phys.* **57** (1985) 965.
- [27] *MAD — Methodical Accelerator Design*, <http://mad.web.cern.ch/mad>.
- [28] A. Friedman et al., *Computational methods in the Warp code framework for kinetic simulations of particle beams and plasmas*, *IEEE Trans. Plasma Sci.* **42** (2014) 1321.
- [29] *Warp*, <http://warp.lbl.gov>.
- [30] J. Amundson, P. Spentzouris, J. Qiang and R. Ryne, *Synergia: An accelerator modeling tool with 3-D space charge*, *J. Comp. Phys.* **211** (2006) 229.
- [31] *Synergia*, <https://synergia.fnal.gov/>.
- [32] A. Romanov, *IOTA optics update: Flexibility for experiments*, talk at the *FAST/IOTA Collaboration Meeting*, Fermi National Accelerator Laboratory, Batavia, IL, U.S.A., 6 June 2017, https://indico.fnal.gov/event/13616/contributions/20559/attachments/13356/17013/20170606_IOTA_update.pptx.
- [33] C. Rubbia, *Microwave radiation from the transverse temperature of an intense electron beam confined by a longitudinal magnetic field*, Tech. Rep., *CERN-EP-77-4*, CERN, Geneva (1977).
- [34] J. Bridges, J. Gannon, E. R. Gray, J. Griffin, F. R. Huson, D. E. Johnson et al., *Fermilab electron cooling experiment: Design report*, Tech. Rep., Fermilab, Batavia IL, U.S.A. (1978). 10.2172/1155428.

- [35] G. Tranquille, *Diagnostics for electron cooled beams*, in proceedings of the *European Workshop on Beam Diagnostics and Instrumentation for Particle Accelerators*, Mainz, Germany, 5–7 May 2003, pp. 110–112.
- [36] R.W. Gould and M.A. LaPointe, *Cyclotron resonance in a pure electron plasma column*, *Phys. Rev. Lett.* **67** (1991) 3685.
- [37] N.C. Luhmann, H. Bindslev, H. Park, J. Sánchez, G. Taylor and C.X. Yu, *Chapter 3: Microwave diagnostics*, *Fusion Sci. Technol.* **53** (2008) 335.
- [38] PROJECT 8 collaboration, *Single electron detection and spectroscopy via relativistic cyclotron radiation*, *Phys. Rev. Lett.* **114** (2015) 162501 [[arXiv:1408.5362](https://arxiv.org/abs/1408.5362)].
- [39] C. Xu, B. Dehning, F.S. Domingues Sousa and E. Griesmayer, *Diamond monitor based beam loss measurements in the LHC*, in proceedings of the *5th International Beam Instrumentation Conference*, Barcelona, Spain, 11–15 September 2016, pp. 82–85.
- [40] A.A. Warner, *Thin sCVD diamond halo/loss monitor*, Tech. Rep., Fermilab Lab Directed Research and Development (LDRD) Proposal (unpublished), 2015.
- [41] S. Szustkowski, S. Chattopadhyay, D.J. Crawford and B.T. Freemire, *Skimmer-nozzle configuration measurements for a gas sheet beam profile monitor*, in proceedings of the *North American Particle Accelerator Conference*, Lansing, Michigan, U.S.A., 2–6 September 2019 pp. 573–575.
- [42] S. Szustkowski, *Nonlinear Integrable Optics Beam Dynamics Experiment and Diagnostics*, Ph.D. thesis, Northern Illinois University, DeKalb, Illinois, U.S.A. (2020).
- [43] G. Stancari, A. Burov, V. Lebedev, S. Nagaitsev, E. Prebys and A. Valishev, *Electron lenses and cooling for the Fermilab Integrable Optics Test Accelerator*, in proceedings of *International Workshop on Beam Cooling and Related Topics*, Newport News, VA, U.S.A., 28 September–3 October 2015, pp. 32–35 [[arXiv:1511.01812](https://arxiv.org/abs/1511.01812)].